Key words: Parkinson's disease; sleep attack; narcolepsy; pergolide; levodopa.

Daytime sleep attacks have been reported in Parkinson's disease (PD) patients on a dopamine agonist or levodopa (L-dopa) treatment. However, the actual prevalence and ultimate significance of sleep attacks in PD remain controversial.[1] Some doubt has been expressed over whether the attack really does occur suddenly and without heralding symptoms in these patients, and it has been hypothesized that sleep attack may be preceded by a sleepiness of which the patients are unaware. Our knowledge of sleep attack in PD is based mainly on reports from the patients or their families. No videographic demonstration of this sleep attack has been reported. We report the clinical and videographic findings of a sleep attack in one PD patient after she took excessive L-dopa and pergolide.

CASE REPORT

A 73-year-old woman was diagnosed as having PD at age 60 when a tremor at rest and hypokinesia developed in her right upper limb. Her initial response to levodopa (carbidopa 10/levodopa 100) 200 mg/day was excellent but was complicated by response fluctuations later in the course of the disease. We increased levodopa to 400 mg/day, although the wearing-off phenomenon occurred. Therefore treatment with pergolide was started when she was 68-years old, and gradually its dose was increased to 500 μg/day. She developed mild hallucinations such as seeing a cat or children in the evening. But at the age of 70, severe wearing- off phenomenon appeared, she could not walk for about 1 hour at 10 AM and 3 PM. Pergolide was gradually increased to 1500 μg/day. However, the on-period with dyskinesia and the severe off-period continued. Accordingly, we tried treatment with cabergoline or selegiline hydrochloride, but we could not continue these drugs because of severe hallucinations. The on-period with dyskinesia sometimes appeared because she frequently took additional levodopa and pergolide without physician approval when she could not move. We tried to keep her dose of medicines appropriate to her condition, but she often took excessive levodopa and pergolide. At the age of 72, she started to have daytime sleep attacks while watching television and eating meals several times per week. At the onset of the sleep attacks, her head would suddenly sag and sometimes hit the table. On other occasions, she would drop a cup or other items that she might be holding. Although she did not notice these symptoms, her family became aware of these sleep attacks when she began to speak slowly. Her family recorded this attack using a cellular phone with a video camera. We concluded that this episode was a sleep attack after viewing the video images, and therefore tried to better control the doses of her medications (levodopa and pergolide). Since then these sleep attacks have not recurred. We believe that these sleep attacks were a side effect of excessive doses of levodopa and pergolide. There was no indication of any prior sleep disorder in terms of the International Classification of Sleep Disorders V. In particular, no anamnestic indications of insomnia, restless legs syndrome, narcolepsy, or sleep apnea could be ascertained. Her EEG findings were normal, and there was no evidence of a sleep stage within 5 minutes or sleep onset REM (SOREM) sleep period. A brain MRI showed no abnormality for her age. SPECT with ECD showed no cerebral deficits. A polysomnographic study and multiple sleep latency test (MSLT) could not be carried out due to her lack of cooperation. HLA-typing (DR2, DQ1) was negative for narcolepsy. The Epworth sleepiness scale (ESS) was three points as scored by the patient but was 15 points on the basis of information from her family

Video Imaging

Her family noticed that she always acted peculiar before a sleep attack. Her daughter took a video of two attacks using a cellular phone with a camera. Thus, these video images are slightly grainy, but we can clearly see the nature of these sleep attacks.

Segment 1.

Her family noticed that she spoke in a sleepy tone. She tried to take a cup, but she could not. She dropped her head and fell into an approximately 30-second sleep episode with waggling of her head. She woke up suddenly. She did not remember anything of what happened.

Segment 2.

She spoke slowly, then suddenly dropped her head backward. She waggled her face and made a silent gesture with her mouth. She made a motion with her left hand on her face after a few seconds. She woke up suddenly. She did not remember anything of what happened.

DISCUSSION

This is the first report of capturing shooting a sleep attack movement on video. Unfortunately, we did not witness this attack or shoot a video in the hospital because her doses of drugs were appropriately modified. The quality of these video images from a cell phone camera was limited, but nonetheless the images had captured well the essence of the sleep attacks. Both video images showed common distinctive features. The patient

behaved in a sleep-like manner, and then lost her body tone. She slept for several tens of seconds, but continued to exhibit some automatic behaviors. She then woke up suddenly. These attacks were frequently seen after taking a meal. We concluded that these attacks were not epilepsy, because her EEG findings showed no epileptic discharge and the sleep attack disappeared after reducing the dose of levodopa and pergolide.

The report of a polysomnographic study showed that the REM latency was shorter in such patients than normal.[2] A report on MSLT documented its shorter latency. There have been some reports of a narcolepsy-like phenotype in patients with Parkinson's disease.[3-5] Her video images resembled narcolepsy clinically, although the sleep attack resolved after reducing her medication. Furthermore, no HLA-typing suggestive of narcolepsy was found.

The role of dopaminergic medications in sleep attack is not understood. Neither functional imaging of the dopamine transporter nor dopamine denervation has demonstrated any correlation between the dopamine system and sleepiness.[1] A weak but significant correlation was, however, found between the daily dose of levodopa, or a levodopa equivalent, and sedation.[1] The recently discovered neuropeptide hypocretin is important in maintaining wakefulness and its deficiency results in narcolepsy/cataplexy.[6] Some studies have found that the cerebrospinal fluid hypocretin-1 levels were normal in PD patients with daytime sleepiness,[7] but hypocretin neurotransmission is affected in PD.[8] 1-methyl-4-phenyl-1,2,3,6-tetrahydropyridine1-methyl-4-phenyl-1,2,3,6-tetrahydropyridine-treated mice have increased amounts of REM sleep.[9] Hyperdopamine exposure induced electrophysiological REM activity in the hippocampal area of mice.[10] Furthermore, a D2 dopamine receptor agonist restored this REM activity.[10] Taken together, these data suggest that this sleep attack phenomenon could be a hypersensitivity or a hyperdose reaction to the D2 receptor.

In these patients with sleep attack, the ESS has been reported to be normal.[11,12] In addition, this patient did not notice her sleep attack and sleepiness. Thus, information from a patient's family is very important for diagnosing a sleep disturbance, particularly sleep attacks in PD patients.

REFERENCES

1. Arnulf I. Excessive daytime sleepiness in parkinsonism. Sleep Med Rev 2005;9:185-200.
2. Ulivelli M, Rossi S, Lombardi C, et al. Polysomnographic characterization of pergolide-induced sleep attacks in idiopathic PD. Neurology 2002;58:462-465.
3. Arnulf I, Bonnet AM, Damier P, et al. Hallucinations, REM sleep, and Parkinson's disease: a medical hypothesis. Neurology 2000; 55:281-288.
4. Moller JC, Stiasny K, Hargutt V, et al. Evaluation of sleep and driving performance in six patients with Parkinson's disease reporting sudden onset of sleep under dopaminergic medication: a pilot study. Mov Disord 2002;17:474-481.
5. Rye DB, Bliwise DL, Dihenia B, Gurecki P. FAST TRACK: daytime sleepiness in Parkinson's disease. J Sleep Res 2000;9:63-69.
6. Overeem S, Mignot E, van Dijk JG, Lammers GJ. Narcolepsy: clinical features, new pathophysiologic insights, and future perspectives. J Clin Neurophysiol 2001;18:78-105.
7. Overeem S, van Hilten JJ, Ripley B, Mignot E, Nishino S, Lammers GJ. Normal hypocretin-1 levels in Parkinson's disease patients with excessive daytime sleepiness. Neurology 2002;58:498-499.
8. Fronczek R, Overeem S, Lee SY, et al. Hypocretin (orexin) loss in Parkinson's disease. Brain 2007;130 (Part 6):1577-1585.
9. Monaca C, Laloux C, Jacquesson JM, et al. Vigilance states in a parkinsonian model, the MPTP mouse. Eur J Neurosci 2004;20: 2474-2478.
10. Dzirasa K, Ribeiro S, Costa R, et al. Dopaminergic control of sleep–wake states. J Neurosci 2006;26:10577-10589.
11. Korner Y, Meindorfner C, Moller JC, et al. Predictors of sudden onset of sleep in Parkinson's disease. Mov Disord 2004;19:1298-1305.
12. Tan EK, Lum SY, Fook-Chong SM, et al. Evaluation of somnolence in Parkinson's disease: comparison with age- and sex-matched controls. Neurology 2002;58:465-468.

The G2019S *LRRK2* Mutation in Brazilian Patients with Parkinson's Disease: Phenotype in Monozygotic Twins

Renato P. Munhoz, MD,[1] Yosuke Wakutani, MD,[2] Connie Marras, MD,[3] Helio A. Teive, MD, PhD,[1] Salmo Raskin, MD, PhD,[4] Lineu C. Werneck, MD, PhD,[1] Danielle Moreno, BSc,[2] Christine Sato, BSc,[2] Anthony E. Lang, MD, FRCPC,[3,5] and Ekaterina Rogaeva, PhD[2,5]*

[1]Movement Disorders Unit, Neurology Service, Hospital de Clínicas, Federal University of Paraná, Curitiba, PR, Brazil; [2]Centre for Research in Neurodegenerative Diseases, University of Toronto, Toronto, Ontario, Canada; [3]Movement Disorders Centre, Toronto Western Hospital, University of Toronto, Toronto, Ontario, Canada; [4]Genetika Laboratory, Curitiba, PR, Brazil; [5]Division of Neurology, Department of Medicine, University Health Network, Toronto, Ontario, Canada

Abstract: **Mutations in the Leucine-Rich Repeat Kinase 2 gene (*LRRK2*) are mainly responsible for idiopathic Parkinson's disease (PD) with either a dominant pattern of**

*Correspondence to: Ekaterina Rogaeva, Centre for Neurodegenerative Diseases, Department of Medicine, University of Toronto, 6 Queen's Park Crescent West, Toronto, Ontario, Canada M5S 3H2. E-mail: ekaterina.rogaeva@utoronto.ca

Received 22 March 2007; Revised 19 May 2007; Accepted 9 October 2007

Published online 12 November 2007 in Wiley InterScience (www.interscience.wiley.com). DOI: 10.1002/mds.21832

Neuropathology 2007; **27**, 331–340 doi:10.1111/j.1440-1789.2007.00787.x

Original Article

Widespread spinal cord involvement in progressive supranuclear palsy

Yasushi Iwasaki,[1] Mari Yoshida,[2] Yoshio Hashizume,[2] Manabu Hattori,[3] Ikuko Aiba[4] and Gen Sobue[1]

[1]Department of Neurology, Nagoya University Graduate School of Medicine, Nagoya, [2]Department of Neuropathology, Institute for Medical Science of Aging, Aichi Medical University, Aichi-gun, [3]Department of Neurology and Neuroscience, Nagoya City University Graduate School of Medical Science, Nagoya, and [4]Department of Neurology, National Hospital Organization Higashi Nagoya National Hospital, Nagoya, Japan

We describe the histopathologic features of spinal cord lesions in 10 cases of progressive supranuclear palsy (PSP) and review the literature. Histologic examination revealed atrophy with myelin pallor in the anterior funiculus and anterolateral funiculus in the cervical and thoracic segments in eight of the 10 cases, whereas the posterior funiculus was well preserved. The degrees of atrophy of the anterior funiculus and the anterolateral funiculus correlated with that of the tegmentum of the medulla oblongata. Myelin pallor of the lateral corticospinal tract was observed in two of the 10 cases. Microscopic observation of the spinal white matter, particularly the cervical segment, revealed a few to several neuropil threads, particularly in the white matter surrounding the anterior horn after Gallyas-Braak (GB) staining or AT-8 tau immunostaining. However, the posterior funiculus was completely preserved from the presence of argyrophilic or tau-positive structures. In the spinal gray matter, widespread distribution of neurons with cytoplasmic inclusions and neuropil threads was observed, particularly in the medial division of the anterior horn and intermediate gray matter, especially in the cervical segment. Globose-type neurofibrillary tangles and pretangles were found. The distribution of GB- or AT-8 tau-positive small neurons and neuropil threads resembled that of the spinal interneurons. In conclusion, the spinal cord, especially the cervical segment, is constantly involved in the pathologic process of PSP. We speculate that spinal interneurons and their neuronal processes, particularly in the medial division of the anterior horn and intermediate gray matter of the cervical segment, are most severely damaged in the PSP spinal cord.

Key words: neuronal inclusion, neuropil threads, progressive supranuclear palsy, spinal cord lesion, tract degeneration.

INTRODUCTION

Progressive supranuclear palsy (PSP) was first described and defined as a clinicopathologic entity by Steele *et al.* in 1964.[1] The neuropathologic features of PSP are neuronal loss and astrocytosis with neurofibrillary tangles (NFTs), which are observed mainly in the basal ganglia, brainstem and cerebellum.[1–3] In addition, abnormal glial cytoskeletal structures such as glial fibrillary tangles (GFTs), including tuft-shaped astrocytes and coiled bodies and neuropil threads, are found around these lesions.[2–5] PSP is considered a discrete clinicopathologic entity;[3–6] however, the pathophysiologic mechanisms underlying the lesions are not completely understood. Although spinal cord abnormalities are generally considered uncommon in cases of PSP,[2] there have been some reports of spinal cord lesions in patients with PSP, and the morphologic changes have been described.[1,7–15] Three notable studies were recently reported,[16–18] and the spinal cord is now considered to be one of the regions involved in PSP. In the present study, we systematically examined the spinal cords in 10 cases of PSP using the Gallyas-Braak (GB) impregnation technique[4,5] and AT-8 tau immunostaining,[19] paying particular attention to the tract degeneration and neuronal and glial tau pathology.

MATERIALS AND METHODS

Ten autopsy cases of PSP from the Institute for Medical Science of Aging, Aichi Medical University, were included

Correspondence: Yasushi Iwasaki, MD, Department of Neurology, Nagoya University Graduate School of Medicine, 65 Tsurumai-cho, Showa-ku, Nagoya 466-8550, Japan. Email: iwasaki@sc4.so-net.ne.jp
Received 4 August 2006; revised and accepted 7 November 2006.

Table 1 Clinical summary of 10 cases of progressive supranuclear palsy

Patient	Sex	Age at onset (years)	Age at death (years)	Disease duration (years)	Brain weight (g)	Clinical symptoms and signs				
						Initial symptom	Gaze palsy	Axial rigidity	Nuchal dystonia	Other neurologic signs
1	F	74	75	2	1120	Gait disturbance	+	+	+	Dementia, frequent falls
2	F	58	62	4	1090	Gait disturbance	+	+	+	Akinesia, dementia, frequent falls
3	F	79	84	4	1090	Gait disturbance	+	+	+	Dementia, frequent falls
4	M	76	81	6	1150	Gait disturbance	+	+	+	Dementia, frequent falls
5	F	66	72	6	1080	Tremor of legs	+	+	+	Dementia, hallucination, Frequent falls
6	M	68	75	7	1120	Dysarthria	+	+	+	Frequent falls
7	M	61	68	7	1060	Gait disturbance	+	+	+	Dementia
8	M	71	78	7	1150	Micrographia	+	+	+	Frequent falls
9	F	60	69	9	980	Gait disturbance	+	+	+	Frequent falls
10	M	67	78	11	1120	Gait disturbance	+	+	+	Tremor, frequent falls

in the present study. All patients had typical clinicopathologic features of PSP in accordance with the National Institute of Neurological Disorders (NINDS) and Society of Progressive Supranuclear Palsy (SPSP) and preliminary NINDS diagnostic criteria.[6,20] Tuft-shaped astrocytes, a disease-specific hallmark of PSP,[4,5] were also identified in the cerebral neocortex and the basal ganglia in all patients. For control, spinal cords were collected from eight autopsied patients judged by neuropathologic examination to be free from neurologic degeneration and who did not have neurologic signs or symptoms. The PSP patients comprised five men and five women (mean age at death, 74.2 ± 6.6 years; range, 62–84 years), and control subjects comprised three men and five women (mean age at death, 70.6 ± 5.1 years; range, 61–76 years). Mean disease duration in the PSP patients was 6.3 ± 2.6 years (range, 2–11 years). Clinical data for the PSP patients, arranged in order of disease duration, are summarized in Table 1.

The entire spinal cord of each patient was fixed in neutral formalin for several weeks. Segmental blocks including cervical, thoracic and lumbosacral segments were embedded in paraffin, and 8-μm-thick horizontal sections were then prepared. For routine neuropathologic examination, sections were processed with hematoxylin and eosin (H&E), Klüver-Barrera (KB), Holzer, Bodian silver and GB stains. Immunohistochemistry was carried out with antibodies against phosphorylation-dependent tau (AT-8, mouse monoclonal, diluted 1:3000; Innogenetics, Ghent, Belgium) and glial fibrillary acidic protein (GFAP, mouse monoclonal, diluted 1:400; DAKO, Glostrup, Denmark). Antibody binding was detected by a labeled streptavidin-biotin (LSAB) method with a DAKO LSAB kit (DAKO). The immunostaining protocol was as described previously.[19]

We assessed atrophy, myelin pallor, gliosis, neuronal loss and the presence of NFTs, GFTs and neuropil threads semiquantitatively. Spinal cord atrophy and myelin pallor were assessed in KB-stained samples. Neuronal loss was assessed in the HE- or KB-stained samples. Neurons in the spinal gray matter were classified as large (approximately >33 μm), medium (approximately > 25 – < 33 μm) or small (approximately < 25 μm), according to results of a previous study.[21] The presence of gliosis was judged from the sections treated with the H&E and Holzer stains and GFAP immunostaining. Typical NFTs were identified by Bodian silver staining. We identified neuronal inclusions, GFTs such as tuft-shaped astrocytes and coiled bodies, and neuropil threads in GB-stained and AT-8-tau immunostained sections. Microscopic fields for at least six different levels of the cervical segment, 12 levels of the thoracic segment and six levels of the lumbosacral segment were observed. Furthermore, we looked for correlation between the medulla oblongata and the spinal cord by observing the changes in many sections. The white matter and gray matter of the spinal cord were subdivided into several regions as shown in Tables 2–5, and respective lesions were assessed by semiquantitative analysis. Atrophy of the medulla oblongata and spinal cord atrophy and myelin pallor were assessed as severe (+++), moderate (++), mild (+), very mild (+/–) or none (–). Neuropil threads in the white and gray matter were evaluated by density as numerous (+++), moderate (++), several (+), a few (+/–) or none (–) in the respective regions. Neurons with cytoplasmic inclusions in the gray matter were counted in the respective regions at each spinal segment and averaged as more than six positive neurons (+++), 3–6 positive neurons (++), 1–3 positive neurons (+), 0–1 positive neurons (+/–) or no positive neurons (–). Spearman's rank correlation coefficient was calculated to assess the relation between pathologic features and between pathologic features and clinical measures. Statistical analysis was performed with Excel 2000 (Microsoft, Redmond, WA, USA) and the add-in software Statcel 2 (OMS, Tokyo, Japan).

Table 2 Histologic features shown by Kluver-Barrera staining in the spinal white matter of progressive supranuclear palsy patients

Patient	Atrophy												Myelin pallor											
	Medulla oblongata		Cervical segment				Thoracic segment			Lumbosacral segment			Cervical segment				Thoracic segment			Lumbosacral segment		
	Ventral	Tegmentum	AF	ALF	LCT	PF	AF	ALF	LCT	PF	AF	ALF	LCT	PF	AF	ALF	LCT	PF	AF	ALF	LCT	PF	AF	ALF	LCT	PF
1	−	‡	‡	‡	−	−	+	+	−	−	−	−	−	−	‡	‡	−	−	+	+	−	−	±	±	−	−
2	−	−	±	±	−	−	±	−	−	−	−	−	−	−	+	+	−	−	+	+	−	−	±	±	−	−
3	−	±	−	−	−	−	−	−	−	−	−	−	−	−	+	−	−	−	−	−	−	−	−	−	−	−
4	−	±	±	±	−	−	±	−	−	−	−	−	−	−	±	±	−	−	−	−	−	−	−	−	−	−
5	−	+	‡	‡	±	−	±	−	−	−	−	−	−	−	‡	‡	−	−	+	±	−	−	−	−	−	−
6	−	−	−	−	−	−	−	−	−	−	−	−	−	−	−	−	−	−	−	−	−	−	−	−	−	−
7	−	+	+	±	−	−	±	−	−	−	−	−	−	−	+	±	−	−	±	±	−	−	−	−	−	−
8	−	‡	‡	‡	±	−	‡	+	±	−	−	−	−	−	‡	‡	+	−	‡	+	±	−	±	−	−	−
9	−	‡	‡	‡	±	−	‡	‡	+	−	±	±	−	−	‡	‡	+	−	‡	‡	+	−	±	±	±	−
10	−	+	+	±	−	−	±	−	−	−	−	−	−	−	+	±	−	−	±	−	−	−	−	−	−	−

+++, severe; ++, moderate; +, mild; ±, very mild; −, none. AF, anterior funiculus includes the anterior corticospinal tract and medial longitudinal fasciculus; ALF, anterolateral funiculus; LCT, lateral corticospinal tract; PF, posterior funiculus.

RESULTS

Histologic findings

In eight of the 10 cases, the anterior funiculus and anterolateral funiculus of the cervical and thoracic segments in the KB-stained sections showed atrophy and myelin pallor (Table 2, Fig. 1). In the anterior funiculus and anterolateral funiculus of the cervical white matter, the degree of atrophy correlated with the degree of myelin pallor (in the anterior funiculus, $r_s = 0.98$ and $P < 0.01$; in the anterolateral funiculus, $r_s = 0.98$ and $P < 0.01$). The macroscopic appearances of the posterior funiculus and gray matter were unremarkable.

Tract degeneration

The degrees of atrophy of the anterior funiculus and the anterolateral funiculus in the cervical white matter correlated with that of the tegmentum of the medulla oblongata (between the tegmentum and the anterior funiculus, $r_s = 0.91$ and $P < 0.01$; between the tegmentum and the anterolateral funiculus, $r_s = 0.98$ and $P < 0.01$). Myelin pallor of the lateral corticospinal tract was seen in two of the 10 cases (Table 2, Fig. 1).

Neuronal loss and gliosis

Mild gliosis was revealed by H&E staining, Holzer staining and GFAP immunostaining in the cervical gray matter, particularly in the medial division of the anterior horn and intermediate gray matter. Although the number of small neurons in the medial division of the anterior horn and intermediate gray matter in the cervical segment appeared moderately decreased in cases of PSP, the number of large motor neurons in the anterior horn was relatively normal. The numbers of neurons in the intermediolateral column, Clarke's column and posterior horn were also normal. The number of neurons of Onufrowicz nucleus was moderately decreased.

Tau pathology

White matter

In the white matter of the PSP spinal cords, a few to several neuropil threads and a few coiled bodies were observed in the anterior funiculus and anterolateral funiculus in all cases (Fig. 2), whereas tuft-shaped astrocytes were not seen in the white matter by GB staining or AT-8 tau immunostaining. Detection of neuropil threads in the spinal white matter by GB staining is summarized in Table 3. Although the density of neuropil threads varied from case to case, these structures were observed most frequently in the white matter surrounding the anterior horn, especially in

Table 3 Number of neuropil threads detected by Gallyas-Braak staining in the spinal white matter of progressive supranuclear palsy patients

Patient	Cervical segment				Thoracic segment				Lumbosacral segment			
	AF	ALF	LCT	PF	AF	ALF	LCT	PF	AF	ALF	LCT	PF
1	±	–	–	–	–	–	–	–	–	–	–	–
2	+	+	–	–	±	–	–	–	–	–	–	–
3	+	±	–	–	±	–	–	–	±	–	–	–
4	+	±	–	–	±	–	–	–	–	–	–	–
5	±	±	–	–	–	–	–	–	–	–	–	–
6	±	±	–	–	±	–	–	–	–	–	–	–
7	±	±	–	–	–	–	–	–	–	–	–	–
8	±	–	–	–	–	–	–	–	–	–	–	–
9	±	–	–	–	±	–	–	–	–	–	–	–
10	±	–	–	–	–	–	–	–	–	–	–	–

+++, numerous; ++, moderate; +, several; ±, a few; –, none. AF, anterior funiculus includes the anterior corticospinal tract and medial longitudinal fasciculus; ALF, anterolateral funiculus; LCT, lateral corticospinal tract; PF, posterior funiculus.

Table 4 Neurons with cytoplasmic inclusions detected by Gallyas-Braak staining in the spinal gray matter of progressive supranuclear palsy patients

Patient	Cervical segment				Thoracic segment			Lumbosacral segment			
	AH		IGM	PH	AH	IGM	PH	AH		IGM	PH
	MD	LD						MD	LD		
1	±	±	+	±	±	+	±	–	–	+	–
2	±	±	+	+	–	–	–	–	–	±	–
3	+	+	+++	+	±	+	±	±	±	+	±
4	+	+	++	+	+	+	+	±	±	±	±
5	±	±	+	±	±	+	±	–	–	±	–
6	+	+	++	+	±	+	±	±	–	±	–
7	±	±	++	+	±	+	±	±	±	+	+
8	+	+	+++	+	±	+	±	±	±	+	±
9	+	+	++	+	±	+	±	±	–	+	±
10	+	+	++	±	±	+	±	±	±	±	±

+++, more than 6 positive neurons; ++, 3-6 positive neurons; +, 1-3 positive neurons; ±, 0-1 positive neurons; –, no positive neuron. AH, anterior horn; IGM, intermediate gray matter; LD, lateral division; MD, medial division; PH, posterior horn.

Table 5 Number of neuropil threads detected by Gallyas-Braak staining in the spinal gray matter of progressive supranuclear palsy patients

Patient	Cervical segment				Thoracic segment			Lumbosacral segment			
	AH		IGM	PH	AH	IGM	PH	AH		IGM	PH
	MD	LD						MD	LD		
1	++	+	+++	±	++	++	±	–	–	±	–
2	+++	++	++	+	±	±	±	–	–	±	–
3	+++	++	+++	+	++	++	+	+	+	++	+
4	+++	++	+++	+	++	++	+	+	+	+	+
5	++	+	++	+	+	+	±	+	+	+	±
6	++	+	++	+	+	++	±	+	±	+	–
7	++	+	++	+	++	++	±	+	+	+	±
8	++	++	++	+	+	+	±	±	±	+	+
9	++	++	+++	+	+	++	+	+	±	+	±
10	+	+	++	±	+	+	±	±	±	+	±

+++, numerous; ++, moderate; +, several; ±, a few; –, none. AH, anterior horn; IGM, intermediate gray matter; LD, lateral division; MD, medial division; PH, posterior horn.

the medial longitudinal fasciculus and the reticular formation of the anterior funiculus. These findings were more conspicuous in the cervical segment than in the thoracolumbosacral segment. In the anterior funiculus and anterolateral funiculus of the cervical white matter, the degree of atrophy did not correlate with the number of neuropil threads (in the anterior funiculus, $r_s = -0.28$ and $P = 0.40$; in the anterolateral funiculus, $r_s = -0.36$ and $P = 0.28$). The

posterior funiculus was completely preserved from the presence of GB- or AT-8 tau-positive structures.

Gray matter

Gallyas-Braak staining and AT-8 tau immunostaining revealed argyrophilic and tau-positive structures including GFTs such as tuft-shaped astrocytes and coiled bodies, numerous neuropil threads and neuronal inclusions in the spinal gray matter (Fig. 3). Detection of neurons with cytoplasmic inclusions and neuropil threads in the spinal gray matter by GB staining is summarized in Tables 4 and 5, respectively. Many argyrophilic or tau-positive neuronal inclusions were observed, particularly in the small neurons in the intermediate gray matter, and such inclusions were relatively sparse in the lateral division of the anterior horn and posterior horn (Fig. 4). These positively stained neurons were observed more frequently in the cervical segment than in the thoracolumbosacral segment. Neither age at onset nor disease duration correlated with the number of neurons with cytoplasmic inclusions in the cervical intermediate gray matter (between age at onset and the number of positive neurons, $r_s = 0.50$ and $P = 0.13$; between the disease duration and the number of positive neurons, $r_s = 0.44$ and $P = 0.18$). Neuronal inclusions were of the globose type, suggestive of NFTs (Fig. 3a), or showed diffuse granular accumulation of cytoplasmic tau, suggestive of pretangles (Fig. 3b). A few neuronal inclusions were seen in the large motor neurons of the anterior horn, intermediolateral column and Clarke's column, and some large motor neurons showed filamentous cytoplasmic inclusions (Fig. 3c). In contrast to the GB-stained and AT-8-immunostained sections, the Bodian silver-stained sections showed a few typical NFTs. The typical NFTs revealed by Bodian silver staining were of the globose type (Fig. 3d) and located mainly in the intermediate gray matter and the basal portion of the posterior horn, but they were not observed in large motor neurons in the anterior horn.

The number of neuropil threads was much greater in the gray matter than in the white matter. The density of neuropil threads varied between patients, but the distribution pattern was relatively uniform and prominent in the medial division of anterior horn and intermediate gray matter (Fig. 5). These conditions were observed more frequently in the cervical segment than in the thoracolumbosacral segment. In the anterior horn of the cervical segment, neuropil threads were prominent in the medial division, and they decreased in density toward the lateral division. In the intermediate gray matter, neuropil threads were prominent in the lateral portion, and they decreased in density toward the medial portion. In the posterior horn, neuropil threads were observed most frequently in the basal portion, and a few were seen in the substantia gelatinosa and the substan-

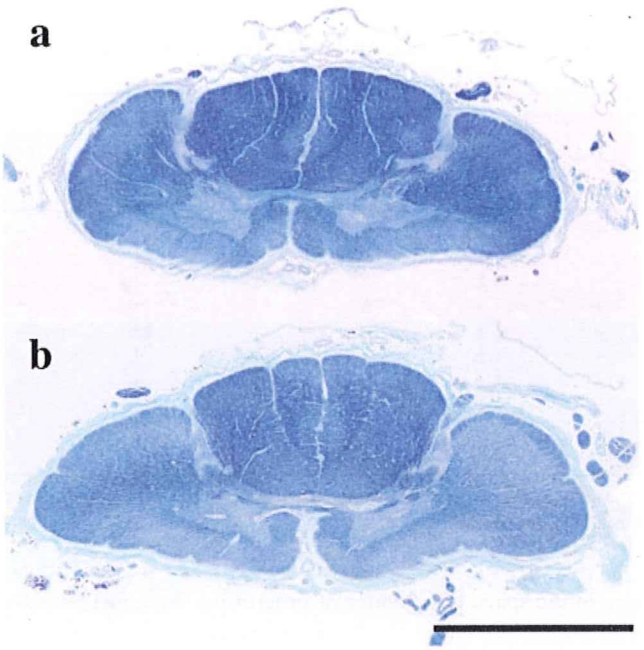

Fig. 1 Representative images of the cervical segments from two patients with progressive supranuclear palsy (PSP). The anterior and anterolateral funiculus showed atrophy and myelin pallor. These two cases also showed myelin pallor of the lateral corticospinal tract (a: patient 8, b: patient 9, Klüver-Barrera staining). Bar = 5 mm.

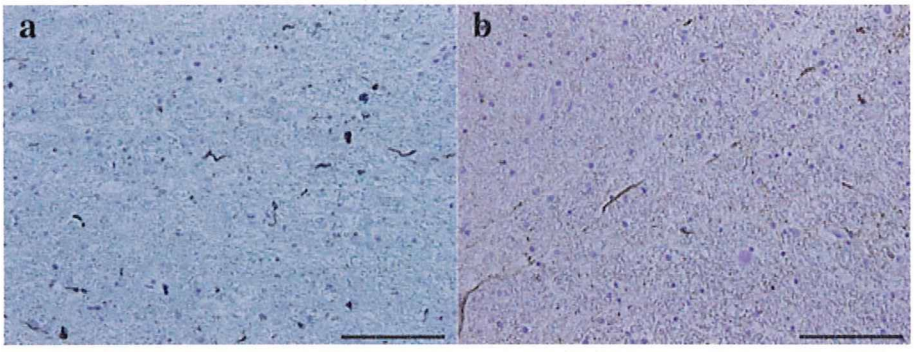

Fig. 2 White matter lesions of the progressive supranuclear palsy (PSP) spinal cord. Several neuropil threads are present in the white matter surrounding the anterior horn (a: patient 4, Gallyas-Braak staining; b: patient 7, AT-8 tau immunostaining). Bars = 100 μm.

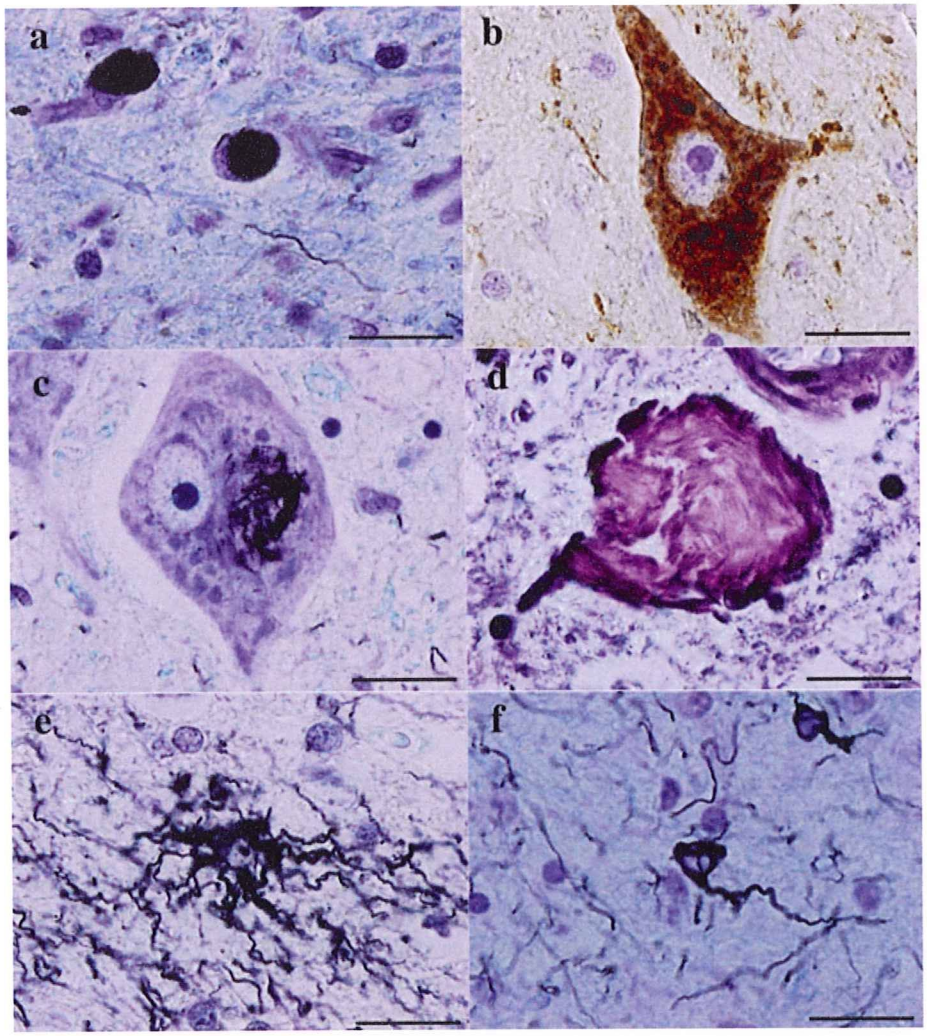

Fig. 3 Representative neuronal inclusions and glial inclusions in the progressive supranuclear palsy (PSP) spinal cord. (a) Globose-type, neurofibrillary tangle (NFT)-like neuronal inclusions in intermediate gray matter in the cervical segment (patient 8, Gallyas-Braak [GB] staining). (b) Pretangle-like neuronal inclusion in a large motor neuron in the anterior horn of the cervical segment (patient 3, AT-8 tau immunostaining). (c) Filamentous cytoplasmic inclusions in a large motor neuron in the anterior horn of the cervical segment (patient 8, GB staining). (d) Typical NFT seen in the basal portion of the posterior horn (patient 3, Bodian silver staining). (e) Tuft-shaped astrocyte in the medial division of the anterior horn in the cervical segment (patient 3, GB staining). (f) Coiled body in the intermediate gray matter in the cervical segment (patient 3, GB staining). Bars = 20 μm.

tia spongiosa. Neither age at onset nor disease duration correlated with the density of neuropil threads in the cervical intermediate gray matter (between age at onset and the density of neuropil threads, $r_s = 0.56$ and $P = 0.09$; between the disease duration and the density of neuropil threads, $r_s = -0.15$ and $P = 0.66$). The density of neuropil threads did not correlate with the number of neurons with cytoplasmic inclusions in the cervical intermediate gray matter (in the medial division of the anterior horn, $r_s = 0.22$ and $P = 0.50$; in the intermediate gray matter, $r_s = 0.30$ and $P = 0.36$). The distribution of small neurons with cytoplasmic inclusions and neuropil threads was similar to that of spinal interneurons and their processes, particularly in the cervical segment.

A few tuft-shaped astrocytes were seen in the spinal gray matter (Fig. 3e), but the distribution could not be assessed because there were so few. A few to several coiled bodies were seen in the spinal gray matter (Fig. 3f); the distribution pattern was almost the same as that of neuropil threads, but they were fewer in number than the neuropil threads.

The number of AT-8 tau-positive structures was much greater than the number of GB-positive argyrophilic structures. No tau-positive or argyrophilic structures were identified in any control spinal cord.

DISCUSSION

In the original PSP report by Steele *et al.*[1] the presence of NFTs in the two examined spinal cords was briefly described. Loss of neurons in the anterior horn[7–10,12,13] and the presence of NFTs in the spinal cord have been described.[1,7,11,14] Kato *et al.* performed ultrastructural electron microscopy studies of NFTs in PSP spinal cords and reported that the NFTs consisted of bundles of straight fibrils with a diameter of approximately 15 nm[22] These NFTs were arranged in bundles of compact parallel arrays and were found to be essentially identical to the NFTs in the brain.[22] The presence of neuropil threads in the spinal white matter was described only by Umahara *et al.*[15] Recently, three notable studies pertaining to PSP spinal cord lesions were reported.[16–18] Kikuchi *et al.* showed

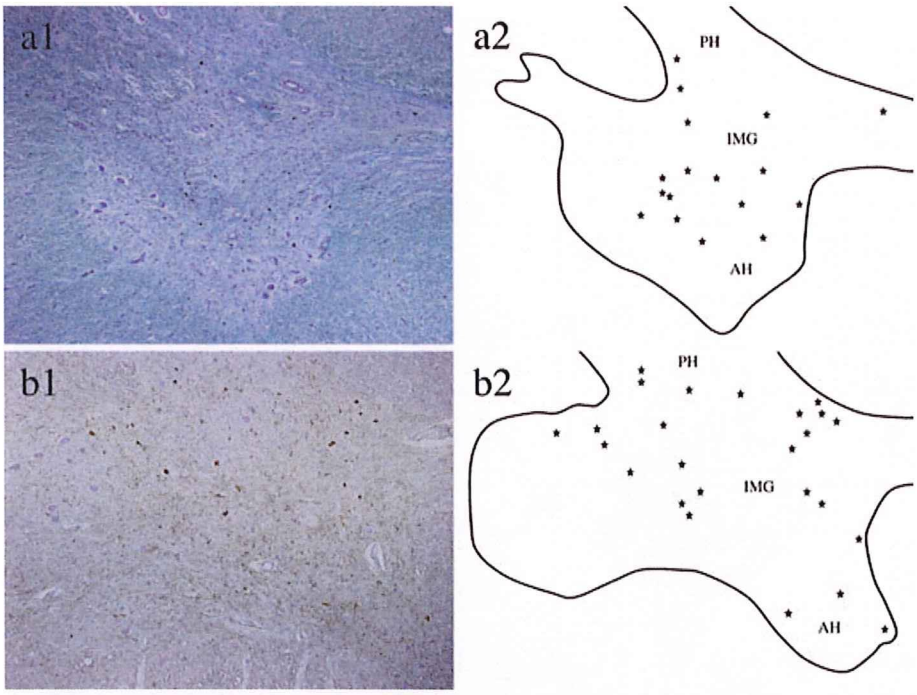

Fig. 4 Identification of neurons with cytoplasmic inclusions in two representative progressive supranuclear palsy (PSP) cases. Many argyrophilic or tau-positive neurons were observed, particularly among the small neurons in the medial division of the anterior horn and intermediate gray matter, and such neurons were relatively sparse in the posterior horn and lateral division of the anterior horn. (a: patient 8, b: patient 3; a1: Gallyas-Braak staining, b1: AT-8 tau immunostaining, a2 and b2 show the schema of a1 and b1, respectively. Asterisks indicate positively stained neurons; cervical segment). (*AH,* anterior hor; *IMG,* intermediate gray matter; *PH,* posterior horn).

by immunohistochemistry that microtubule-associated protein-2 expression in the cervical segment was significantly decreased in the medial division of the anterior horn, intermediate gray matter and posterior horn but that there was no significant change in the substantia gelatinosa or lateral division of the anterior horn.[16] Scaravilli *et al.* investigated the Onufrowicz nucleus in three cases of PSP and found neuronal loss and the presence of NFTs, glial inclusions and neuropil threads.[17] Vitaliani *et al.* reported severe neuronal loss throughout the spinal cord in five cases of PSP.[18]

Brainstem lesions have been regarded as the primary PSP lesions.[1] Murakami *et al.* confirmed correlation between tract degeneration of the tegmentum of the medulla oblongata and that of the anterolateral funiculus of the cervical segment of the PSP spinal cord.[23] Similar tract degeneration was observed in the present study, and atrophy and myelin pallor of the anterior funiculus and anterolateral funiculus were also observed. Two of the 10 cases showed myelin pallor of the lateral corticospinal tract, indicating pyramidal tract degeneration in PSP. Interestingly, although the degree of atrophy correlated with the degree of myelin pallor, the degrees of atrophy and myelin pallor did not correlate with the number of neuropil threads in the cervical white matter. We think this discrepancy is due to the fact that tract degeneration seen in PSP-affected spinal white matter is secondary degeneration due to the tegmental involvement of the brainstem, particularly in the medulla oblongata. Furthermore, although a few to several neuropil threads were observed mainly in the anterior funiculus and anterolateral funiculus in the PSP-affected spinal white matter, argyrophilic- or tau-positive structures were completely absent in the posterior funiculus. We speculate that this discrepancy may reflect centrifugal spread of tau pathology along the descending fibers or regional susceptibility for tau accumulation in the PSP spinal cord.

The most important finding of the present study was the identification of widespread neurons with cytoplasmic inclusions and neuropil threads in the PSP spinal cord, particularly in the cervical gray matter. Subdivision of the spinal gray matter according to Rexed's schema allowed us to determine that neurons with cytoplasmic inclusions and neuropil threads were abundant in the Rexed VI, VII and VIII layers.[24] Spinal gray matter lesions did not necessarily coexist with prominent spinal white matter lesions. The number of neurons with cytoplasmic inclusions and the density of neuropil threads did not correlate with age at onset or with disease duration. These neurons, positive for GB staining or AT-8 tau immunostaining, were mostly small neurons in the medial division of the anterior horn and intermediate gray matter and could not be easily detected by Bodian silver staining. Therefore, we speculate that most neurons with cytoplasmic inclusions, which were positive for GB staining and AT-8 tau immunostaining, were immature pretangles.[19,25] Although the density of neuropil threads and the number of neurons with cytoplasmic inclusions in the spinal gray matter varied from case to case, these features were common to all cases of PSP. Because no tau-positive structures or argyrophilic struc-

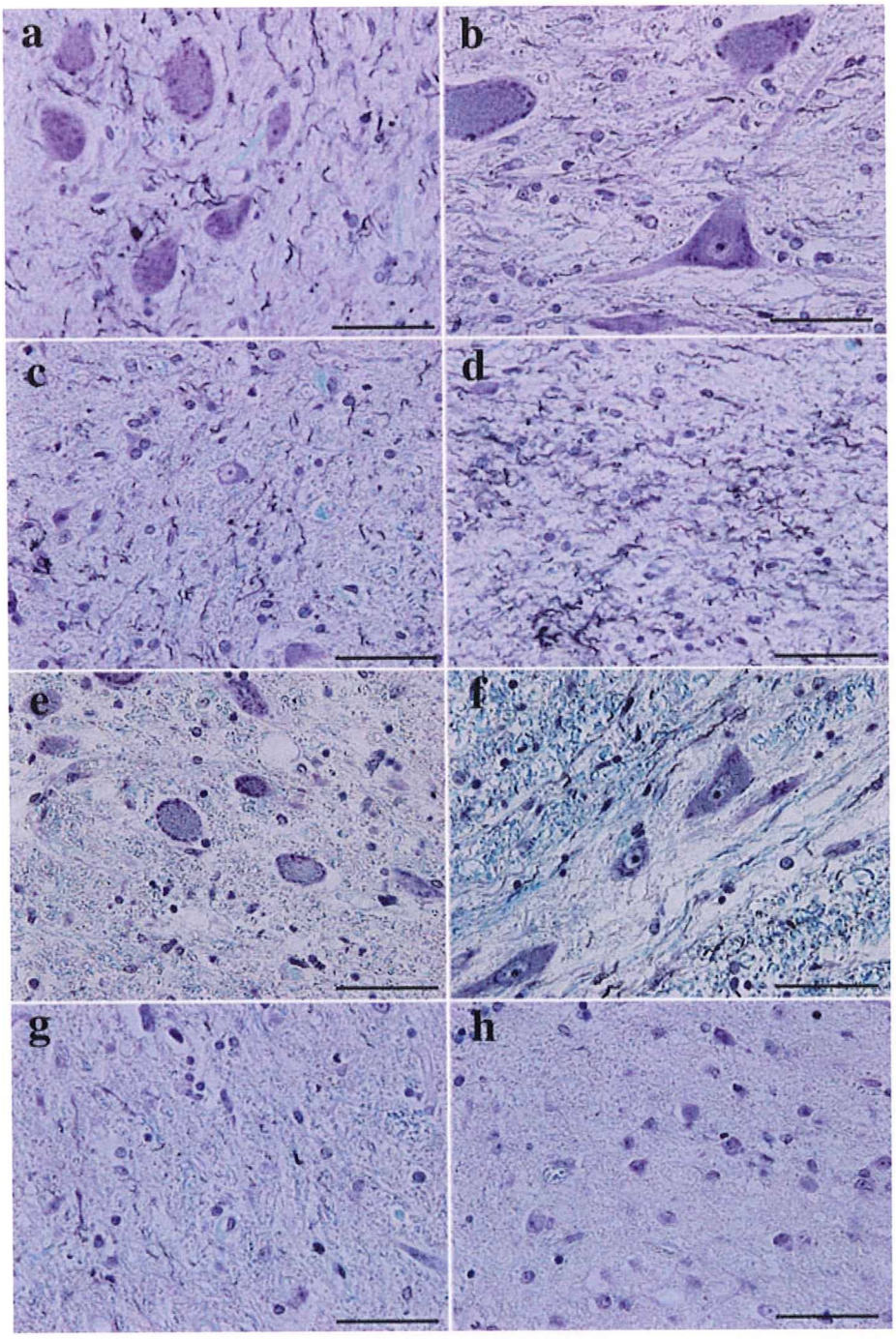

Fig. 5 Presence of neuropil threads in the gray matter lesions. (a) Medial division of the anterior horn in the cervical segment. (b) Lateral division of the anterior horn in the cervical segment. (c) Medial portion of the intermediate gray matter in the cervical segment. (d) Lateral portion of the intermediate gray matter in the cervical segment. (e) Intermediolateral column in the upper thoracic segment. (f) Clarke's column in the upper thoracic segment. (g) Basal portion of the posterior horn in the cervical segment. (h) Substantia gelatinosa of the posterior horn in the cervical segment (patient 3, Gallyas-Braak staining). Bars = 50 μm.

tures were identified in the eight control spinal cords, our results indicate that the PSP spinal cord is affected by an abnormal tau-degenerative alteration. Some authors have argued that tuft-shaped astrocytes are characteristic of PSP,[4–6,20] but only a few tuft-shaped astrocytes were seen in some PSP spinal cords in the present study.

The relation between the pathologic features of spinal cord lesions and clinical signs of PSP is not well understood. In the anterior horn of the cervical segment, passing from the most medial part to its lateral periphery, motor neurons successively innervate muscles of the trunk, shoulder, upper arm, forearm and fingers.[26] The small neurons, which are distributed in the intermediate gray matter of the spinal cord, comprise mainly interneurons.[26,27] It is noteworthy that the distribution of small neurons with cytoplasmic inclusions and neuropil threads was well matched with that of spinal interneurons and their neuronal processes in the cervical segment. The descending fibers of the extrapyramidal system, such as those of the rubrospinal tract, tectospinal tract, reticulospinal tract and

medial longitudinal fasciculus, synapse with interneurons that connect to motor neurons of the anterior horn[26,27] and the spinal interneurons that mediate between input and output elements and produce varied reflex behaviors.[28] Therefore, we also speculate that these spinal gray matter lesions, particularly in the medial division of the anterior horn and intermediate gray matter of the cervical segment, cause the nuchal dystonia, retrocollis and axial rigidity characteristic of PSP patients. Similar speculation was made by Kikuchi *et al.*[16] but Vitaliani *et al.* concluded that this hypothesis could not be supported by their data.[18] Further neuropathologic investigation is needed to elucidate the underlying relations between spinal cord lesions and clinical signs of PSP.

Important findings in the present study include atrophy and myelin pallor of the anterior funiculus and anterolateral funiculus and the existence of white matter and gray matter lesions including the presence of GB- and AT-8 tau-positive cytoskeletal structures, particularly in the cervical segment. Widespread spinal cord involvement as seen in the present study suggests the presence of tract degeneration and damage of the spinal interneurons and their neuronal processes. We emphasize that these spinal cord lesions, especially in the cervical segment, should be included in the list of pathologic lesions of PSP.

REFERENCES

1. Steele JC, Richardson JC, Olszewski J. Progressive supranuclear palsy: a heterogeneous degeneration involving the brain stem, basal ganglia and cerebellum with vertical gaze and pseudobulbar palsy, nuchal dystonia and dementia. *Arch Neurol* 1964; **10**: 333–359.
2. Lowe JS, Leigh N. Disorder of movement and system degenerations. In: Graham DI, Lantos PL, eds. *Greenfield's Neuropathology*, 7th edn. London: Arnold, 2002; 337–342.
3. Duvoison RC. Progressive supranuclear palsy. In: Rowland LP, ed. *Merritt's Textbook of Neurology*, 9th edn. Baltimore, MD: Williams & Wilkins, 1995; 730–733.
4. Iwasaki Y, Yoshida M, Hattori M *et al.* Distribution of tuft-shaped astrocytes in the cerebral cortex in progressive supranuclear palsy. *Acta Neuropathol (Berl)* 2004; **108**: 399–405.
5. Hattori M, Hashizume Y, Yoshida M *et al.* Distribution of astrocytic plaques in the corticobasal degeneration brain and comparison with tuft-shaped astrocytes in the progressive supranuclear palsy brain. *Acta Neuropathol (Berl)* 2003; **106**: 143–149.
6. Hauw JJ, Daniel SE, Dickson D *et al.* Preliminary NINDS neuropathologic criteria for Steel–Richardson–Olszewski syndrome (progressive supranuclear palsy). *Neurology* 1994; **44**: 2015–2019.
7. Behrman S, Carroll JD, Janota I, Matthews WB. Progressive supranuclear palsy: clinicopathological study of four cases. *Brain* 1969; **92**: 663–678.
8. Blumenthal H, Miller C. Motor nuclear involvement in progressive supranuclear palsy. *Arch Neurol* 1969; **20**: 362–367.
9. Bugiani O, Mancardi GL, Brusa A, Ederli A. The fine structure of subcortical neurofibrillary tangles in progressive supranuclear palsy. *Acta Neuropathol (Berl)* 1979; **45**: 147–152.
10. Ishino H, Higashi H, Kuroda S, Yabuki S, Hayahara T, Otsuki S. Motor nuclear involvement in progressive supranuclear palsy. *J Neurol Sci* 1974; **22**: 235–244.
11. Kato T, Hirano A, Weinberg MN, Jacobs AK. Spinal cord lesion in progressive supranuclear palsy: some new observations. *Acta Neuropathol (Berl)* 1986; **71**: 11–14.
12. Kurihara T, Landau WM, Torack RM. Progressive supranuclear palsy with action myoclonus, seizure. *Neurology* 1974; **24**: 219–223.
13. Powell HC, London GW, Lampert PW. Neurofibrillary tangles in progressive supranuclear palsy: electron microscopic observations. *J Neuropathol Exp Neurol* 1974; **33**: 98–106.
14. Tomonaga M. Ultrastructure of neurofibrillary tangles in progressive supranuclear palsy. *Acta Neuropathol (Berl)* 1977; **37**: 177–181.
15. Umahara T, Hirano A, Kato S, Shibata N, Yen SC. Demonstration of neuropil thread-like structures in the spinal cord white matter in progressive supranuclear palsy: an immunohistochemical investigation. *Neuropathology* 1995; **15**: 103–107.
16. Kikuchi H, Doh-ura K, Kira J, Iwai T. Preferential neurodegeneration in the cervical spinal cord of progressive supranuclear palsy. *Acta Neuropathol (Berl)* 1999; **97**: 577–584.
17. Scaravilli T, Pramstaller PP, Salerno A *et al.* Neuronal loss in Onuf's nucleus in three patients with progressive supranuclear palsy. *Ann Neurol* 2000; **48**: 97–101.
18. Vitaliani R, Scaravilli T, Egarter-Vigl E *et al.* The pathology of the spinal cord in progressive supranuclear palsy. *J Neuropathol Exp Neurol* 2002; **61**: 268–274.
19. Iwasaki Y, Yoshida M, Hattori M, Hashizume Y, Sobue G. Widespread spinal cord involvement in corticobasal degeneration. *Acta Neuropathol (Berl)* 2005; **109**: 632–638.
20. Litvan I, Agid Y, Calne D *et al.* Clinical research criteria for the diagnosis of progressive supranuclear palsy (Steel–Richardson–Olszewski syndrome): report of

the NINDS-SPSP international workshop. *Neurology* 1996; **47**: 1–9.
21. Terao S, Sobue G, Hashizume Y, Mitsuma T, Takahashi A. Disease-specific patterns of neuronal loss in the spinal ventral horn in amyotrophic lateral sclerosis, multiple system atrophy and X-linked recessive bulbospinal neuronopathy, with special reference to the loss of small neurons in the intermediate zone. *J Neurol* 1994; **241**: 196–203.
22. Kato S, Hirano A, Llena JF. Immunohistochemical, ultrastructural and immunoelectron microscopic studies of spinal cord neurofibrillary tangles in progressive supranuclear palsy. *Neuropathol Appl Neurobiol* 1992; **18**: 531–538.
23. Murakami N, Yoshida M, Aiba I, Hashizume Y. *Neuropathological characteristics of anterolateral funiculus of spinal cord of progressive supranuclear palsy (PSP) – in comparison with amyotrophic lateral sclerosis.* Annual report of the research committee of CNS degenerative disease, Ministry of Health and Welfare of Japan, 1995; 210–213 (in Japanese with English Abstract).
24. Rexed B. A cytoarchitectonic atlas of the spinal cord in the cat. *J Comp Neurol* 1954; **100**: 297–351.
25. Iwatsubo T, Hasegawa M, Ihara Y. Neuronal and glial tau-positive inclusions in diverse neurologic diseases share common phosphorylation characteristic. *Acta Neuropathol (Berl)* 1994; **88**: 129–136.
26. Andre P. Spinal cord: regional anatomy and internal structure. In: Andre P, ed. *Carpenter's Human Neuroanatomy*, 9th edn. Baltimore, MD: Williams & Wilkins, 1996; 325–367.
27. Kuypers HG. A new look at the organization of the motor system. *Prog Brain Res* 1982; **57**: 381–403.
28. Kandel ER, Schwarz JH, Jessell TM. *Principles of Neural Science*, 3rd edn. Amsterdam: Elsevier, 1991.

ELSEVIER

Journal of the Neurological Sciences 263 (2007) 133 – 138

Journal of the Neurological Sciences

www.elsevier.com/locate/jns

Clinical Research Paper

Dobutamine stress test unmasks cardiac sympathetic denervation in Parkinson's disease

Tomohiko Nakamura [a], Masaaki Hirayama [a], Hiroki Ito [a], Motoko Takamori [a], Kensuke Hamada [b], Shigeo Takeuchi [b], Hirohisa Watanabe [a], Yasuo Koike [c], Gen Sobue [a,*]

[a] *Department of Neurology, Nagoya University Graduate School of Medicine, 65 Tsurumai-cho, Showa-ku, Nagoya 466-8550, Japan*
[b] *Department of Neurology, Aichi-ken Saiseikai Hospital, 1-1-18 Sako, Nishi-ku, Nagoya 451-0052, Japan*
[c] *Department of Health Science, Nagoya University Graduate School of Medicine, 1-1-20 Daikominami, Higashi-ku, Nagoya 461-8673, Japan*

Received 3 April 2007; received in revised form 22 June 2007; accepted 3 July 2007
Available online 1 August 2007

Abstract

Objective: Cardiac uptake of [^{123}I]metaiodobenzyl guanidine (MIBG) is reduced in patients with Parkinson's disease (PD). However, the cardiac sympathetic abnormality associated with this reduction is unclear. To unmask this abnormality in PD patients we examined the functional consequences of cardiac beta-receptor activation.
Methods: Cardiovascular responses to stepwise administration of the beta1-receptor agonist, dobutamine (DOB), were assessed in 25 PD patients and 12 age-matched controls. Changes in blood pressure were compared to determine the optimal dose at which to detect denervation supersensitivity, and cardiac contractility was measured by DOB echocardiography, based on peak aortic flow velocity. The relations of these cardiovascular responses to the ratio of MIBG uptake into the heart vs. that into the mediastinum (H/M ratio) were analyzed.
Results: At 4 μg/kg/min DOB, systolic blood pressure increased more in PD patients than in controls (PD, 17.5±12.3 mm Hg; control, 7.2± 6.2 mm Hg, $p<0.01$), suggesting the presence of denervation supersensitivity. At this DOB dose cardiac contractility also increased more in PD than in controls (PD, 39.0±15.7%; control, 23.5±5.2%, $p<0.005$) and this hyperdynamic response was significantly correlated with reduced H/M ratios (early: $r=-0.63$, $p<0.01$, delayed: $r=-0.66$, $p<0.01$).
Conclusion: Low-dose DOB unmasks cardiac sympathetic denervation in PD patients, and decreased MIBG uptake indicates the presence of denervation supersensitivity within the heart, resulting in hyperdynamic cardiac contractility in response to a beta 1-stress condition.

Keywords: Parkinson's disease; Dobutamine; Denervation supersensitivity; Cardiac sympathetic denervation; Dobutamine echocardiography; MIBG; Cardiac contractility

1. Introduction

Since Hakusui first demonstrated cardiac sympathetic nerve damage in patients with Parkinson's disease (PD) by decreased cardiac [^{123}I]metaiodobenzyl guanidine (MIBG) uptake [1], a large number of studies have documented this phenomenon [2–4]. Uptake of MIBG reflects myocardial sympathetic nerve function [5]. Histological assessment of the sympathetic nerve axon population innervating cardiac muscle is also markedly decreased in PD patients and is considered to account for the decrease in MIBG uptake [6,7]. Severe abnormal MIBG findings in peripheral vessels were also found in PD with autonomic failure [8]. However, the cardiac sympathetic abnormality correlated to reduced MIBG uptake in PD patients has not been clarified. Echocardiography has demonstrated normal ventricular systolic function under resting conditions in PD patients [9].

Cardiovascular responses to sympathomimetic agents have been anecdotally described to be exaggerated in PD patients [10,11] but it is unclear whether these responses are due to impaired cardiac sympathetic nerve function or other

* Corresponding author. Tel.: +81 52 744 2385; fax: +81 52 744 2384.
E-mail address: sobueg@med.nagoya-u.ac.jp (G. Sobue).

0022-510X/$ - see front matter © 2007 Elsevier B.V. All rights reserved.
doi:10.1016/j.jns.2007.07.005

peripheral/central autonomic system abnormalities. Dobutamine (DOB) is a synthetic sympathomimetic amine that directly stimulates beta-adrenergic receptors, especially beta1-receptors [12,13]. In normal subjects, infusion of DOB in doses up to 10 μg/kg/min increases cardiac output and heart rate (HR) but has little effect on blood pressure (BP) [13,14]. DOB is commonly used in the stress test to diagnose ischemic heart disease [15,16]. Specifically, low-dose DOB has been used, because it is safe and convenient to administer, to identify viable myocardial impairment [17,18].

In PD patients, various degrees of primary chronic autonomic failure are seen and some patients with orthostatic hypotension display evidence of cardiac sympathetic denervation [19]. Thus, it is clinically important to clarify how this cardiac denervation correlates with the decreased MIBG uptake that is commonly seen in PD patients. The purpose of this study was to assess the cardiovascular response of beta1-adrenergic receptors using low-dose DOB to detect cardiac denervation supersensitivity and unmask the cardiac abnormality associated with decreased MIBG uptake in patients with PD. Echocardiography was performed to evaluate the cardiac response to DOB and verify the association between this response and the degree of cardiac MIBG uptake.

2. Subjects and methods

2.1. Subjects

We included 25 patients with PD (10 men, 15 women) who were referred to the Nagoya University Hospital. PD was diagnosed according to the United Kingdom Parkinson's Disease Society Brain Bank Clinical Diagnosis Criteria [20]. All patients underwent precise neurological examinations and brain MRIs to exclude diagnoses other than PD. In all cases, no obvious heart disease, including experience of anginal pain, or diabetes mellitus was detected and electrocardiographs were all normal. The mean patient age was 65.5±8.1 and the mean duration since the onset of symptoms was 4.8±3.7 years (range: 1 to 12 years; Table 1). The control subjects were normal healthy volunteers (5 men, 7 women, 61.1±14.0 years old) with no history of heart disease, diabetes mellitus, or intracranial disease and no obvious abnormalities observed on physical examination. Orthostatic hypotension was absent during head-up tilt testing in the control group. Informed consent was obtained from all participants and the protocol of the study was approved by the ethics committee of Nagoya University Graduate School of Medicine.

2.2. DOB infusion test

Patients abstained from eating and the use of anti-parkinsonian drugs on the morning of testing. No patient took other drugs that might influence BP responses, such as midodorine or droxidopa. The subjects were tested in the supine position. After resting for at least 5 min, DOB (2 μg/kg/min; 0.5 ml/min) was administered by continuous intravenous infusion via a brachial venous cannula using a constant infusion pump. After 5 min the infusion was increased to 4 μg/kg/min and continued for another 5 min until: (1) the systolic BP (SBP) was > 170 mm Hg or the SBP increase was > 40 mm Hg, or (2) the HR > 100/min, or (3) there was an increase in the frequency of arrhythmias, or (4) the development of untoward side effects. BP and HR were recorded every minute with an automated sphygmomanometer (BP-508, Nippon Colin, Tokyo, Japan), designed for autonomic studies, placed on the upper arm opposite to that used for the DOB infusion. The electrocardiogram was monitored continuously throughout the procedure.

Table 1
Clinical characteristics

	PD (n=25)	Control (n=12)	p value
Age (years)	65.5 (8.1)	61.1 (14.0)	N.S.
Gender (M/F)	10/15	5/7	N.S.
Disease duration (years)	4.8 (3.7)		
Hoehn and Yahr stages	I:3; II:6; III:8; IV:8		
Levodopa (mg/day)	254.8 (190.4)		

Values are expressed as mean (±SD). PD=Parkinson's disease; N.S.=not significant.

2.3. Echocardiographic examination

DOB echocardiography of Doppler examinations were performed using a Hewlett Packard Sonos 1500 ultrasound system (Andover, MA) with 1.9 MHz (Pedoff) transducers. The entire exam was performed by a single investigator who did not know the results of the MIBG scintigraphy. The aortic flow velocity (AFV) waveform was acquired by continuous-wave Doppler from the supraclavicular fossa and angled toward the ascending aorta. Peak AFV was used to evaluate changes in cardiac contractility [21]. Monitoring of the aortic flow wave using echocardiography was performed 3 min after each incremental DOB infusion. When sharp, well-defined velocity waveforms were seen on the monitor and maximal pitch was heard through the integral loudspeaker, a 5-s recording was "frozen" on-screen and measurements were made directly from the monitor using a built-in light pen system with dedicated software.

2.4. MIBG scintigraphy

MIBG (111 mBq) was injected intravenously into each subject. The early image of cardiac uptake was obtained 15 min later and the delayed image was obtained after 3 or 4 h. Regions of interest included the whole heart and mediastinum in the anterior projection. The ratio of MIBG uptake by the heart to that in the mediastinum (H/M ratio)

Table 2
Cardiovascular response to DOB

	Baseline	DOB dosage	
		2 μg/kg/min	4 μg/kg/min
PD (n=25)			
SBP (mm Hg)	122.1 (13.8)	125.3 (16.9)*	139.6 (21.3)****
DBP (mm Hg)	69.6 (10.4)	69.9 (11.9)	72.9 (12.8)
HR (bpm)	68.9 (10.8)	67.9 (11.4)	72.4 (13.4)**
Controls (n=12)			
SBP (mm Hg)	121.4 (17.8)	123.7 (18.4)	128.6 (18.5)**
DBP (mm Hg)	70.2 (9.9)	68.6 (10.0)	67.4 (8.4)
HR (bpm)	63.7 (8.3)	63.7 (9.8)	68.0 (9.2)***

Values are expressed as mean (±SD). DOB=dobutamine; SBP=systolic blood pressure; DBP=diastolic blood pressure; HR=heart rate; bpm=beats per minute. *p<0.05 vs. baseline; **p<0.01 vs. baseline; ***p<0.005 vs. baseline; and ****p<0.0001 vs. baseline.

was calculated, and ratios from early and delayed images were evaluated.

2.5. Data analysis and statistics

Data are expressed as means (±SD). For evaluating the pharmacokinetic actions of DOB, the average values for BP and HR during the last 3 min of infusion were used for analysis. However, if the infusion was stopped in the middle of the protocol, then data from just before discontinuing the infusion were used for analysis. Supersensitive responses for the hemodynamic changes were defined as changes greater than 2 standard deviations from the mean. Tables of frequency data were examined using Fisher's exact probability test. Individual data were analyzed using the Mann–Whitney's U test between groups and by Wilcoxon's signed rank test within the groups. Relationships with the H/M ratio were analyzed using Spearman's correlation coefficient. Calculations were performed using the statistical software package StatView (Abacus Concepts, Berkeley, CA). The level of significance was defined at $p<0.05$.

3. Results

3.1. Appropriate dose of DOB to detect a supersensitive response in PD patients

There were no significant differences in baseline cardiovascular measurements between the PD patients and the control subjects (Table 2). During the 2 μg/kg/min DOB infusion, the mean SBP increased significantly in the PD subjects but not in control subjects; no significant changes in mean diastolic BP (DBP) or HR changes were observed in either group. During the 4 μg/kg/min DOB infusion, mean SBP increased another 14.3 mm Hg in the PD subjects but the increase was only slight in control subjects. No significant DBP change was seen in either group at this dose. HR increased in both groups.

All control subjects completed the entire procedure. All PD patients also completed the procedure, however, six (24%) had met our withdrawal criteria by the end of the 4 μg/kg/min dose of DOB (1 with SBP >170 mm Hg, 1 with SBP

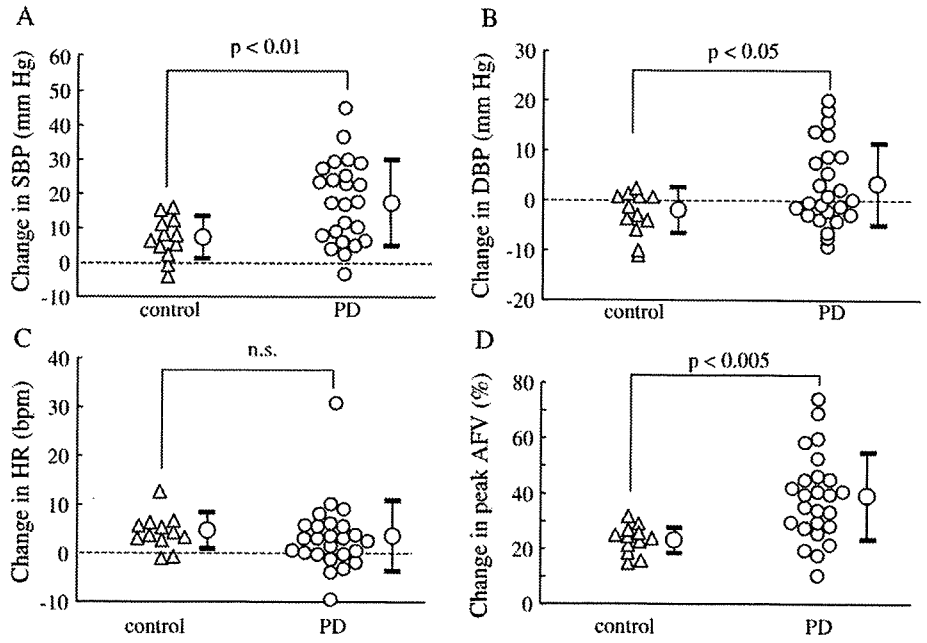

Fig. 1. Changes in SBP, DBP, HR, and peak AFV after infusion of 4 μg/kg/min DOB in controls and PD patients. (A) The mean change in SBP is significantly greater in the PD group than in the control group. (B) There was also a significant difference in the DBP change between the PD and control groups. (C) No difference was seen in the HR change between the groups. (D) The mean percentage change in peak AFV was significantly larger in the PD group than in the control group. SBP: systolic blood pressure, DBP: diastolic blood pressure, HR: heart rate, DOB: dobutamine, AFV: aortic flow velocity, PD: Parkinson's disease. n.s.=not significant.

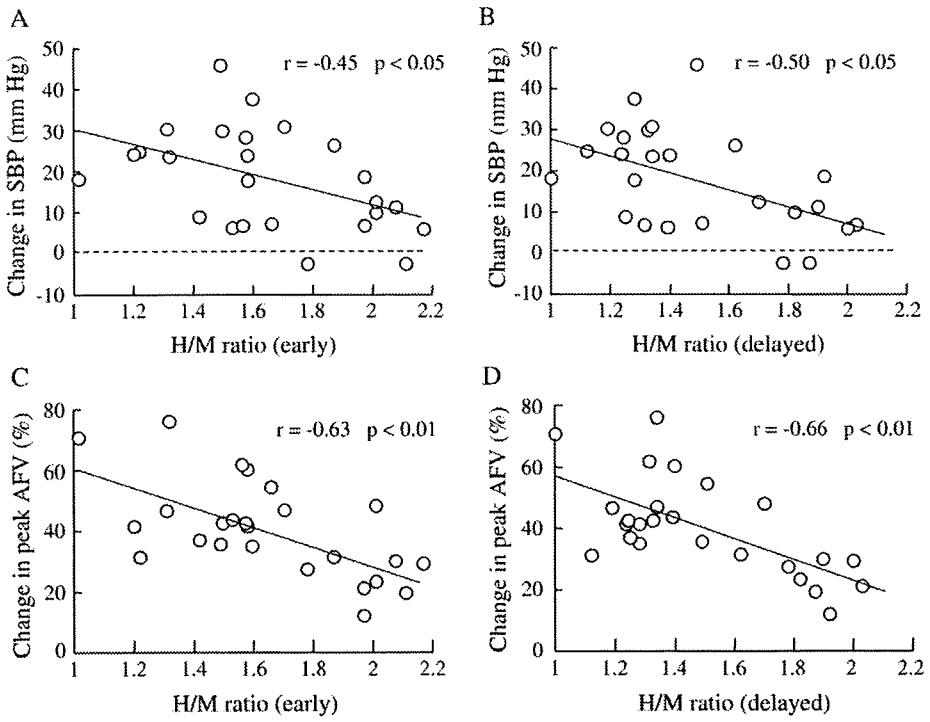

Fig. 2. Correlation between changes in SBP and peak AFV during infusion of 4 μg/kg/min DOB and the H/M ratios in patients with PD. Significant correlations between SBP changes and (A) the early image H/M ratio and (B) the delayed H/M ratio were observed. Significant correlations between changes in peak AFV and (C) early H/M ratio and (D) delayed H/M ratio were observed. SBP: systolic blood pressure, AFV: aortic flow velocity, DOB: dobutamine, PD: Parkinson's disease.

change >40 mm Hg, 1 with HR > 100/min, 1 with ventricular premature complexes, and 2 with urge to urinate). These responses were all transient and normalized within a few minutes. As many more patients experienced hyperdynamic responses after the 4 μg/kg/min dose of DOB than during the 2 μg/kg/min dose, we decided that the 4 μg/kg/min dose of DOB was the optimal dose for observing hyperdynamic cardiovascular responses.

3.2. Comparison of hemodynamic changes in control subjects and PD subjects after infusion of 4 μg/kg/min DOB

Changes from baseline in SBP, DBP, and HR are shown in Fig. 1. The increase in SBP was significantly larger in the PD patients than in the control subjects, indicating the presence of denervation supersensitivity (PD, 17.5±12.3 mm Hg; control, 7.2±6.2 mm Hg, $p<0.01$; Fig. 1A). Eleven PD patients (44%) demonstrated such a supersensitive reaction (SBP increase more than 20 mm Hg) to an infusion of 4 μg/kg/min DOB. There was also a significantly larger change in DBP in the PD subjects than in the controls (PD, 3.2±8.2 mm Hg; control, −2.8±4.5 mm Hg, $p<0.05$; Fig. 1B). There were no significant differences in the HR changes between the two groups (PD, 3.5±7.2 bpm; control, 4.3±3.6 bpm, $p=0.35$; Fig. 1C). Peak AFV increased 39.0±15.7% (range: 10.7% to 74.6%) in the PD group and 23.5±5.2% (range: 14.7 to 31.8%) in controls; the change in the PD patients being significantly larger than that in the controls ($p<0.005$; Fig. 1D).

3.3. Correlation between the MIBG H/M ratio and cardiovascular responses after infusion of 4 μg/kg/min DOB

MIBG scintigraphy was performed in all PD patients. The mean MIBG H/M ratio of the early images, obtained 15 min after injection of MIBG, was 1.65±0.31 (range: 1.02 to 2.17). Delayed images made 3–4 h later showed a mean MIBG H/M ratio of 1.49±0.30 (range: 1.00 to 2.38). Fifteen patients had H/M ratios <1.5 in the delayed images and 10 (67%) of these patients had supersensitive reactions to 4 μg/kg/min of DOB, while 8 patients with H/M ratios > 1.7 in the delayed images all showed no supersensitive reactions. The relationships between MIBG H/M ratios and hemodynamic changes during administration of 4 μg/kg/min DOB are shown in Fig. 2. The mean increase in SBP was inversely correlated with both the early and delayed H/M ratios (Fig. 2A, B). The change in peak AFV also showed a significant negative correlation with the H/M ratios (Fig. 2C, D).

4. Discussion

This is the first study to illustrate that a hyperdynamic cardiac response due to beta1-mediated cardiac supersensitivity, assessed by an excessive increase in BP and cardiac contractility, was present during DOB infusion, and furthermore, to elucidate that this cardiac response was significantly correlated to decreased MIBG uptake in patients with PD. Decreases in the MIBG H/M ratio in PD patients represent beta-adrenergic cardiac supersensitivity, leading to

hyperdynamic cardiac contractility. This hyperdynamic cardiac contractility is not obvious under resting conditions, but does manifest itself under beta-adrenergic stress.

The presence of denervation supersensitivity is usually evaluated by observing changes in SBP or HR, and in our study SBP observation proved useful in the evaluation of cardiac sympathetic denervation. However, a hyperdynamic pressor response was not observed in about one-third of the patients who exhibited decreased MIBG uptake. This is likely to be the consequence of the influence of peripheral vascular resistance. In addition to cardiac contractility, vascular resistance also contributes considerably to SBP. DOB also has slight vasoconstriction and vasodilatation effects due to its action at alpha1- and beta2-receptors, respectively [12,13]. However, the involvement of systemic vascular resistance in the present SBP changes is not clear. There is a possibility that the increases in SBP were due to the increase of systemic vascular resistance, and that the SBP decreases were due to systemic vascular vasodilatation. Therefore, in order to more accurately evaluate the functional consequences of DOB-induced beta-receptor activation on cardiac responses, we added DOB stress echocardiography to our examination. Evaluating myocardial contractility by measuring peak AFV has certain advantages for demonstrating cardiac denervation. Peak AFV was reported to be influenced predominantly by cardiac inotropic changes [22], while the effects of physical loading are minimal [21]. Furthermore, measurement of peak AFV by Doppler ultrasound is a well-validated, noninvasive method for monitoring cardiac function [21,23]. Patients with decreased MIBG uptake demonstrated hyperdynamic AFV responses in our study. Similar hyperdynamic responses were also reported in patients with cardiac syndrome X [24]. These patients were also reported to have decreased MIBG uptake, and the presence of cardiac adrenergic nerve dysfunction was suggested [25]. These results support our findings showing a strong correlation between decreased MIBG uptake and increased cardiac contractility induced by DOB infusion. We are aware that peak AFV is not a very sophisticated measure for evaluating cardiac contractility. In general, the most frequently used, noninvasive index of left ventricular performance is ejection fraction [18]. However, to demonstrate this, a change in position, such as to the left lateral recumbent position, may be necessary, and it was expected to be difficult for PD patients to maintain such an unstable position for several minutes. Thus, to obtain a stabilized aortic waveform in the completely supine position, we carried out the evaluation from the supraclavicular fossa in our study.

Other factors may also have influenced our results. We took into consideration the influence of levodopa treatment on the cardiovascular response to DOB because hypertension, reflecting the presence of excessive amounts of catecholamines formed from levodopa, has been observed in some patients receiving the drug [26], even though the development of hypotension is much more common [27,28]. However, isoproterenol, a beta-receptor agonist resembling DOB in its action, sensitivity evaluated by a chronotropic response was similar in levodopa-treated and not-treated PD patients, and peripheral beta-adrenergic sensitivity is reported to be unaffected by levodopa treatment [29]. In addition, abnormal regurgitations (atrial, mitral, and tricuspid) are associated with ergot-derived dopamine receptor agonists [30–32]. Valvular changes may also affect the AFV monitored by DOB echocardiography. However, valvular changes are usually observed during high cumulative doses or long-term treatment with these agonists [33]. In our preliminary results, the cardiovascular responses of the patients who were never treated with levodopa or ergot-derived dopamine agonists, or were taking only 100 mg/day levodopa, were also inversely correlated with the H/M ratio (early: ΔSBP; $r=-0.64$, $p<0.05$, cardiac contractility; $r=-0.69$, $p<0.05$, delayed: ΔSBP; $r=-0.69$, $p<0.05$, cardiac contractility; $r=-0.69$, $p<0.05$) (data not shown) and these were similar to the results obtained from the full population. Together, these results seem to indicate that the cardiovascular effects of levodopa or ergot-derived dopamine receptor agonist treatment did not influence our results.

HR is generally considered a good indicator of beta1 cardiac innervation[12,13,34]. However, in only 1 of the 25 patients was it necessary to terminate the DOB procedure due to elevated HR (>100 beats/min). Overall, changes in HR were small, and during the 4 μg/kg/min infusion, there was no significant difference between the changes in PD patients and those in control subjects. At this low dose, it may be speculated that HR is accelerated by direct effects of the drug, but it is also suppressed due to a reflex cardiodeceleration secondary to the elevation in BP. Thus HR does not appear to be a proper marker for detecting beta1-receptor denervation supersensitivity with DOB.

In conclusion, our data demonstrating an exaggerated cardiovascular response to beta-adrenergic stimulation clearly confirm the pathological and nuclear medicine findings of cardiac sympathetic denervation in patients with PD. In particular, we found that a greater decrease in cardiac uptake of MIBG occurred along with a greater DOB-induced hyperdynamic response in cardiac contractility. This study documents that the beta1-adrenergic system is perturbed, and that resulting cardiac denervation is present in PD patients.

Acknowledgments

We thank the inspecting engineer Mrs. Akiko Noda and cardiologist Dr. Akira Yamada for their support with echocardiography.

References

[1] Hakusui S, Yasuda T, Yanagi T, Tohyama J, Hasegawa Y, Koike Y, et al. A radiological analysis of heart sympathetic functions with meta-[^{123}I] iodobenzylguanidine in neurological patients with autonomic failure. J Auton Nerv Syst 1994;49:81–4.

[2] Yoshita M. Differentiation of idiopathic Parkinson's disease from striatonigral degeneration and progressive supranuclear palsy using iodine-123 meta-iodobenzylguanidine myocardial scintigraphy. J Neurol Sci 1998;155:60–7.

[3] Satoh A, Serita T, Seto M, Tomita I, Satoh H, Iwanaga K, et al. Loss of ^{123}I-MIBG uptake by the heart in Parkinson's disease: assessment of cardiac sympathetic denervation and diagnostic value. J Nucl Med 1999;40:371–5.
[4] Hamada K, Hirayama M, Watanabe H, Kobayashi R, Ito H, Ieda T, et al. Onset age and severity of motor impairment are associated with reduction of myocardial ^{123}I-MIBG uptake in Parkinson's disease. J Neurol Neurosurg Psychiatry 2003;74:423–6.
[5] Kline RC, Swanson DP, Wieland DM, Thrall JH, Gross MD, Pitt B, et al. Myocardial imaging in man with I-123 meta-iodobenzylguanidine. J Nucl Med 1981;22:129–32.
[6] Orimo S, Ozawa E, Oka T, Nakade S, Tsuchiya K, Yoshimoto M, et al. Different histopathology accounting for a decrease in myocardial MIBG uptake in PD and MSA. Neurology 2001;57:1140–1.
[7] Orimo S, Oka T, Miura H, Tsuchiya K, Mori F, Wakabayashi K, et al. Sympathetic cardiac denervation in Parkinson's disease and pure autonomic failure but not in multiple system atrophy. J Neurol Neurosurg Psychiatry 2002;73:776–7.
[8] Hirayama M, Hakusui S, Koike Y, Ito K, Kato T, Ikeda M, et al. A scintigraphical qualitative analysis of peripheral vascular sympathetic function with meta-[^{123}I]iodobenzylguanidine in neurological patients with autonomic failure. J Auton Nerv Syst 1995;53:230–4.
[9] Orimo S, Ozawa E, Nakade S, Sugimoto T, Mizusawa H. (123)I-metaiodobenzylguanidine myocardial scintigraphy in Parkinson's disease. J Neurol Neurosurg Psychiatry 1999;67:189–94.
[10] Senard JM, Valet P, Durrieu G, Berlan M, Tran MA, Montastruc JL, et al. Adrenergic supersensitivity in parkinsonians with orthostatic hypotension. Eur J Clin Invest 1990;20:613–9.
[11] Niimi Y, Ieda T, Hirayama M, Koike Y, Sobue G, Hasegawa Y, et al. Clinical and physiological characteristics of autonomic failure with Parkinson's disease. Clin Auton Res 1999;9:139–44.
[12] Tuttle RR, Mills J. Dobutamine: development of a new catecholamine to selectively increase cardiac contractility. Circ Res 1975;36:185–96.
[13] Ruffolo RR. The pharmacology of dobutamine. Am J Med Sci 1987;294:244–8.
[14] Beregovich J, Bianchi C, D'Angelo R, Diaz R, Rubler S. Haemodynamic effects of a new inotropic agent (dobutamine) in chronic cardiac failure. Br Heart J 1975;37:629–34.
[15] Sawada SG, Segar DS, Ryan T, Brown SE, Dohan AM, Williams R, et al. Echocardiographic detection of coronary artery disease during dobutamine infusion. Circulation 1991;83:1605–14.
[16] Barasch E, Wilansky S. Dobutamine stress echocardiography in clinical practice with a review of the recent literature. Tex Heart Inst J 1994;21:202–10.
[17] Neskovic AN, Otasevic P. Stress-echocardiography in idiopathic dilated cardiomyopathy: instructions for use. Cardiovasc Ultrasound 2005;3:3.
[18] Gorcsan J, Deswal A, Mankad S, Mandarino WA, Mahler CM, Yamazaki N, et al. Quantification of the myocardial response to low-dose dobutamine using tissue Doppler echocardiographic measures of velocity and velocity gradient. Am J Cardiol 1998;81:615–23.
[19] Goldstein DS, Holmes C, Li ST, Bruce S, Metman LV, Cannon RO. Cardiac sympathetic denervation in Parkinson disease. Ann Intern Med 2000;133:338–47.
[20] Gibb WR, Lees AJ. The relevance of the Lewy body to the pathogenesis of the idiopathic Parkinson's disease. J Neurol Neurosurg Psychiatry 1988;51:745–52.
[21] Hsieh KS, Chang CK, Chang KC, Chen HI. Effect of loading conditions on peak aortic flow velocity and its maximal acceleration. Proc Natl Sci Counc Repub China B 1991;15:165–70.
[22] Singer M, Allen MJ, Webb AR, Bennett ED. Effects of alterations in left ventricular filling, contractility, and systemic vascular resistance on the ascending aortic blood velocity waveform of normal subjects. Crit Care Med 1991;19:1138–45.
[23] Huntsman LL, Stewart DK, Barnes SR, Franklin SB, Colocousis JS, Hessel EA. Noninvasive Doppler determination of cardiac output in man. Clinical validation. Circulation 1983;67:593–602.
[24] Madaric J, Bartunek J, Verhamme K, Penicka M, Van Schuerbeeck E, Nellens P, et al. Hyperdynamic myocardial response to beta-adrenergic stimulation in patients with chest pain and normal coronary arteries. J Am Coll Cardiol 2005;46:1270–5.
[25] Lanza GA, Giordano A, Pristipino C, Calcagni ML, Meduri G, Trani C, et al. Abnormal cardiac adrenergic nerve function in patients with syndrome X detected by [^{123}I]metaiodobenzylguanidine myocardial scintigraphy. Circulation 1997;96:821–6.
[26] Watanabe AM, Parks LC, Kopin IJ. Modification of the cardiovascular effects of L-dopa by decarboxylase inhibitors. J Clin Invest 1971;50:1322–8.
[27] Wolf JP, Bouhaddi M, Louisy F, Mikehiev A, Mourot L, Cappelle S, et al. Side-effects of L-dopa on venous tone in Parkinson's disease: a leg-weighing assessment. Clin Sci (Lond) 2006;110:369–77.
[28] Bouhaddi M, Vuillier F, Fortrat JO, Cappelle S, Henriet MT, Rumbach L, et al. Impaired cardiovascular autonomic control in newly and long-term-treated patients with Parkinson's disease: involvement of L-dopa therapy. Auton Neurosci 2004;116(1-2):30–8.
[29] Durrieu G, Rispail Y, Chatelut E, Berlan M, Rascol A, Montastruc JL, et al. Beta-adrenergic sensitivity in Parkinson's disease: effect of levodopa treatment. Clin Neuropharmacol 1990;13:492–9.
[30] Van Camp G, Flamez A, Cosyns B, Goldstein J, Perdaens C, Schoors D. Heart valvular disease in patients with Parkinson's disease treated with high-dose pergolide. Neurology 2003;61:859–61.
[31] Van Camp G, Flamez A, Cosyns B, Weytjens C, Muyldermans L, Van Zandijcke M, et al. Treatment of Parkinson's disease with pergolide and relation to restrictive valvular heart disease. Lancet 2004;363:1179–83.
[32] Zanettini R, Antonini A, Gatto G, Gentile R, Tesei S, Pezzoli G. Valvular heart disease and the use of dopamine agonists for Parkinson's disease. N Engl J Med 2007;356:39–46.
[33] Yamamoto M, Uesugi T, Nakayama T. Dopamine agonists and cardiac valvulopathy in Parkinson disease: a case-control study. Neurology 2006;67:1225–9.
[34] Baser SM, Brown RT, Curras MT, Baucom CE, Hooper DR, Polinsky RJ. Beta-receptor sensitivity in autonomic failure. Neurology 1991;41:1107–12.

THE JOURNAL OF BIOLOGICAL CHEMISTRY VOL. 282, NO. 38, pp. 28087–28095, September 21, 2007

Disulfide Bond Mediates Aggregation, Toxicity, and Ubiquitylation of Familial Amyotrophic Lateral Sclerosis-linked Mutant SOD1*[S]

Received for publication, May 31, 2007, and in revised form, July 13, 2007 Published, JBC Papers in Press, July 31, 2007, DOI 10.1074/jbc.M704465200

Jun-ichi Niwa[‡§], Shin-ichi Yamada[‡], Shinsuke Ishigaki[‡], Jun Sone[‡], Miho Takahashi[‡], Masahisa Katsuno[‡], Fumiaki Tanaka[‡], Manabu Doyu[‡§], and Gen Sobue[‡1]

From the [‡]Department of Neurology, Nagoya University Graduate School of Medicine, 65 Tsurumai-cho, Showa-ku, Nagoya 466-8500 and the [§]Stroke Center, Aichi Medical University, Aichi 480-1195, Japan

Mutations in the Cu/Zn-superoxide dismutase (*SOD1*) gene cause familial amyotrophic lateral sclerosis (ALS) through the gain of a toxic function; however, the nature of this toxic function remains largely unknown. Ubiquitylated aggregates of mutant SOD1 proteins in affected brain lesions are pathological hallmarks of the disease and are suggested to be involved in several proposed mechanisms of motor neuron death. Recent studies suggest that mutant SOD1 readily forms an incorrect disulfide bond upon mild oxidative stress *in vitro*, and the insoluble SOD1 aggregates in spinal cord of ALS model mice contain multimers cross-linked via intermolecular disulfide bonds. Here we show that a non-physiological intermolecular disulfide bond between cysteines at positions 6 and 111 of mutant SOD1 is important for high molecular weight aggregate formation, ubiquitylation, and neurotoxicity, all of which were dramatically reduced when the pertinent cysteines were replaced in mutant SOD1 expressed in Neuro-2a cells. Dorfin is a ubiquityl ligase that specifically binds familial ALS-linked mutant SOD1 and ubiquitylates it, thereby promoting its degradation. We found that Dorfin ubiquitylated mutant SOD1 by recognizing the Cys^6- and Cys^{111}-disulfide cross-linked form and targeted it for proteasomal degradation.

Cu/Zn superoxide dismutase (SOD1),[2] a major intracellular antioxidant enzyme, metabolizes superoxide radicals to molecular oxygen and hydrogen peroxide (1, 2). Because mutations in *SOD1* linked to familial amyotrophic lateral sclerosis (ALS) were first identified (3), more than 100 mutations at over 70 residues in the 153-amino acid SOD1 protein have been reported (4). Most mutations are missense mutations, with a few causing early termination or frame shifts near the carboxyl terminus of the protein. *SOD1* mutations account for ~20% of familial ALS, which is characterized by selective degeneration of motor neurons. SOD1 is primarily a cytosolic protein (5), and the active enzyme is a homodimer of two subunits (6). Each subunit contains four cysteine (Cys) residues at positions 6, 57, 111, and 146. An intramolecular disulfide bond between Cys^{57} and Cys^{146} of each subunit facilitates its correct folding and stabilizes the active homodimeric structure (7, 8), but it is not known how the disulfide is formed in the reducing environment of the cytosol. Although the endoplasmic reticulum is the specialized site for oxidative folding (9), there is no SOD1 localization to the endoplasmic reticulum (10). Most familial ALS-linked mutations render SOD1 more susceptible to intramolecular disulfide bond reduction (11) and accelerate the rate of protein turnover (12, 13). Recent lines of evidence implicate the disulfide-reduced monomer as the common aggregation-prone, neurotoxic intermediate of mutant SOD1 proteins (8, 11, 14–16), and a significant fraction of the insoluble SOD1 aggregates in the spinal cord of mutant SOD1 transgenic mice contains high molecular weight species cross-linked via intermolecular disulfide bonds (17). Hence, modulation of disulfide bond formation may be important in mutant SOD1-linked motor neuron-selective neurotoxicity.

ALS-linked mutant SOD1 proteins are turned over more rapidly than wild-type SOD1, and proteasome inhibitors increase the amount of mutant SOD1 (18, 19). To date, two distinct ubiquityl ligases, Dorfin and NEDL1, have been reported to ubiquitylate mutant SOD1 (20, 21). Dorfin is a RING-finger/IBR (in-between ring-finger) domain-containing ubiquityl ligase, which we previously identified from human spinal cord (22), and belongs to the RBR (RING-Between rings-RING) family of proteins (23). Dorfin physically binds and ubiquitylates various familial ALS-linked SOD1 mutants and subsequently targets them for proteasomal degradation, but it has no effect on the stability of wild-type SOD1 (20). Overexpression of Dorfin protects neuronal cells against the toxic effects of mutant SOD1 and reduces the number of aggregates composed of mutant SOD1 (20). However, the mechanism by which Dorfin discriminates between the normal and pathogenic status of SOD1 proteins remains unknown. There are numerous variants causing familial ALS, thus it seems reasonable that Dorfin recognizes a common protein modification among mutant SOD1s that is not present in wild-type SOD1.

* This work was supported by a Center of Excellence grant from the Ministry of Education, Culture, Sports, Science and Technology and grants from the Ministry of Health, Labor and Welfare of Japan. The costs of publication of this article were defrayed in part by the payment of page charges. This article must therefore be hereby marked "*advertisement*" in accordance with 18 U.S.C. Section 1734 solely to indicate this fact.

[S] The on-line version of this article (available at http://www.jbc.org) contains supplemental Fig. S1.

[1] To whom correspondence should be addressed. Tel.: 81-52-744-2385; Fax: 81-52-744-2384; E-mail: sobueg@med.nagoya-u.ac.jp.

[2] The abbreviations used are: SOD1, superoxide dismutase 1; ALS, amyotrophic lateral sclerosis; 2-ME, 2-mercaptoethanol; WST-1, 4-[3-(4-iodophenyl)-2-(4-nitrophenyl)-2H-5-tetrazolio]-1,3-benzene disulfonate; GFP, green fluorescent protein.

In this study, we generated SOD1 proteins with various combinations of the four Cys residues replaced by serines and assessed their disulfide bond status, the changes in the formations of their high molecular weight species, and their neurotoxicity. Moreover, by studying the interaction between Dorfin and these engineered SOD1s, we investigated whether disulfide bonds are critical for Dorfin recognition and ubiquitylation of mutant SOD1s.

EXPERIMENTAL PROCEDURES

Construction of Expression Vectors—Construction of pcDNA3.1/MycHis-SOD1, pEGFP-N1-SOD1, and pcDNA4/HisMax-Dorfin vectors were described previously (20, 22). Cys to Ser missense mutations were introduced into pcDNA3.1/MycHis-SOD1 and pEGFP-N1-SOD1 with a QuikChange site-directed mutagenesis kit (Stratagene, La Jolla, CA). Primer pairs for each Cys to Ser mutant were as follows: 5′-CGAAGGCCGTGTCCGTGCTGAAGGGC-3′ and 5′-GCCCTTCAGCACGGACACGGCCTTCG-3′ for C6S; 5′-GATAATACAGCAGGCTCTACCAGTGCAGGTCC-3′ and 5′-GGACCTGCACTGGTAGAGCCTGCTGTATTATC-3′ for C57S; 5′-CTCAGGAGACCATTCCATCATTGGCCGCAC-3′ and 5′-GTGCGGCCAATGATGGAATGGTCTCCTGAG-3′ for C111S; and 5′-GGAAGTCGTTTGGCTTCTGGTGTAATTGGGATCG-3′ and 5′-CGATCCCAATTACACCAGAAGCCAAACGACTTCC-3 for C146S. Multiple Cys to Ser replaced vectors were obtained by repeatedly applying a mutagenesis.

Cell Culture, Transfection, and Antibodies—Neuro-2a cells (American Type Culture Collection, Manassas, VA), a line derived from mouse neuroblastoma, were maintained in Dulbecco's modified Eagle's medium containing 10% fetal calf serum, 5 units/ml penicillin, and 50 μg/ml streptomycin. Transfections were performed using Lipofectamine 2000 (Invitrogen) in the WST-1 assay or Effectene Transfection Reagent (Qiagen, Valencia, CA) in other experiments according to the manufacturers' instructions. To inhibit cellular proteasome activity, cells were treated with 1 μM (except as otherwise indicated) MG132 (Z-Leu-Leu-Leu-al, Sigma) or epoxomicin (Sigma) as indicated concentration for 24 h after overnight transfection. To differentiate Neuro-2a cells, they were changed to Dulbecco's modified Eagle's medium culture medium containing 2% fetal calf serum and 20 μM retinoic acid and cultured for 48 h. Primary antibodies used were as follows: anti-Myc mouse monoclonal antibody (9E10, Sigma), anti-Myc rabbit polyclonal antibody (A-14, Santa Cruz Biotechnology, Santa Cruz, CA), anti-SOD1 rabbit polyclonal antibody (SOD100, Stressgen Bioreagents, Victoria, Canada), anti-α-tubulin mouse monoclonal antibody (B-5-1-1, Sigma), anti-ubiquitin mouse monoclonal antibody (4PD1, Santa Cruz Biotechnology), and anti-Xpress mouse monoclonal antibody (Invitrogen).

Transgenic Mice—17-week-old symptomatic B6SJL-TgN(SOD1-G93A)1Gur ALS mice overexpressing the human mutant $SOD1^{G93A}$ (The Jackson Laboratory, Bar Harbor, ME) were used. The experimental design of this study was fully approved by the Experimental Animal Ethical Committee of the Nagoya University Graduate School of Medicine. Tissues were homogenized in 10 volumes of lysis buffer (TNE) consisting of 50 mM Tris-HCl, 150 mM NaCl, 1% Nonidet P-40, and 1 mM EDTA with a protease inhibitor mixture (Complete Mini, Roche Diagnostics, Indianapolis, IN) and centrifuged at 20,000 × *g* for 30 min at 4 °C. Supernatants were used for Western blotting analysis.

Immunoprecipitation and Western Blotting Analysis—5×10^5 cells from a 6-cm dish were lysed on ice with 1 ml of TNE lysis buffer. The lysate was centrifuged at 1,000 × *g* for 15 min at 4 °C to remove nuclei and cell debris. Denucleated cell lysates (crude fraction) were separated into supernatant (soluble fraction) and pellet fractions by centrifuging at 20,000 × *g* for 20 min at 4 °C. The pellets were lysed (insoluble fraction) with 1 ml of TNES lysis buffer consisting of 50 mM Tris-HCl, 150 mM NaCl, 1% Nonidet P-40, 2% SDS, and 1 mM EDTA with a protease inhibitor mixture (Complete Mini, Roche Diagnostics). Protein concentrations were determined with a DC protein assay kit (Bio-Rad). Immunoprecipitation from the soluble fraction was performed with 2 μg of anti-Myc or anti-Xpress antibodies and Protein A/G Plus-agarose (Santa Cruz Biotechnology), and the precipitates were washed four times in TNE buffer. Cell lysates or immunoprecipitates were separated by SDS-PAGE (5–20% gradient gel) and analyzed by Western blotting with ECL plus detection reagents (GE Healthcare Bio-Sciences, Piscataway, NJ). Non-reducing SDS-PAGE was conducted without 2-mercaptoethanol (2-ME) in the sample buffer. Because omitting reducing agents from the protein samples can lead to adventitious air oxidation or disulfide scrambling, 100 mM iodoacetamide was added to the lysates to prevent these changes during sample preparation.

Filter Trap Assay—Each of the various fractions from the cell lysates (crude, soluble, and insoluble fractions) was filtered under vacuum through 0.2-μm cellulose acetate membranes (Sartorius, Gottingen, Germany) followed by two washes in Tris-buffered saline. The membranes were then incubated with 5% milk powder in Tris-buffered saline at room temperature for 1 h, followed by an overnight incubation at 4 °C with anti-Myc antibody in Tris-buffered saline with 0.1% Tween 20. Primary antibodies were detected with horseradish peroxidase-conjugated secondary antibodies (GE Healthcare Bio-Sciences), which were then detected with ECL plus chemiluminescence reagent (GE Healthcare Bio-Sciences). To confirm equal loading of proteins, the same samples were blotted onto 0.45-μm nitrocellulose membranes (Bio-Rad) and probed with anti-Myc or anti-α-tubulin antibodies.

Neurotoxicity Analysis and Quantification of SOD1 Aggregates—2×10^4 Neuro-2a cells were grown overnight on four-chamber, collagen-coated slides (Nalge Nunc, Rochester, NY) and then transfected with 0.2 μg of pEGFP-N1-SOD1. After overnight incubation, the cells were differentiated in Dulbecco's modified Eagle's medium containing 2% fetal calf serum and 20 μM retinoic acid for 48 h. Inclusion bodies were counted in more than 100 randomly selected cells, and the percentages of cells with such inclusions were calculated. Data from three independent experiments were averaged. For the cell viability assay, 5×10^3 Neuro-2a cells were grown in 96-well collagen-coated plates overnight, and then transfected with 0.1 μg of pEGFP-N1-SOD1 or pcDNA3.1/MycHis-SOD1, with or without 0.1 μg of pcDNA4/HisMax-Dorfin. pcDNA4/HisMax